We are IntechOpen,
the world's leading publisher of
Open Access books
Built by scientists, for scientists

6,900
Open access books available

185,000
International authors and editors

200M
Downloads

154
Countries delivered to

Our authors are among the

TOP 1%
most cited scientists

12.2%
Contributors from top 500 universities

BOOK CITATION INDEX
CLARIVATE ANALYTICS
INDEXED

WEB OF SCIENCE™

Selection of our books indexed in the Book Citation Index
in Web of Science™ Core Collection (BKCI)

Interested in publishing with us?
Contact book.department@intechopen.com

An Opaque Solar Lumber Drying House Covered by a Composite Surface

Kanayama Kimio[1], Koga Shinya[2], Baba Hiromu[3] and Sugawara Tomoyoshi[4]
[1]Kitami Institute of Technology
[2]Kyushu University
[3]Formerly, Kitami Institute of Technology
[4]Marusho-giken Co., Ltd.
Japan

1. Introduction

Since old time, natural air drying technique had been utilized in several areas of the world before artificial drying methods for wood were developed. In Hokkaido, Japan, a research on the modified type, in place of the natural air dryer, was developed as a practical technology. For instance, the solar dryers of greenhouse-type and solar house-type were made by hand or constructed architecturally. After tested at the public institute, some of the apparatus were distributed to some areas of northern part of Hokkaido. For several decades, from just after the first energy crisis 1973 until the recent time, as an application of solar radiation in the field of forest industry, an active-type and a semi passive-type of solar wood dryers have been developed experimentally and constructed annually. For instance, a semi passive-type handmade solar lumber dryer was invented by the Hokkaido Forest Industry Product Institute, which occupied one era in a wide area as an auxiliary lumber dryer. Recently, in order to suppress the global warming, a policy to reduce emission of carbon dioxide was urgently required on the worldwide. For example, an artificial steam-type lumber drying emits a lot of carbon dioxide because it consumes a lot of fossil oil, i.e., about fifty liters per one cubic meters of wood.

In this chapter therefore, in drying process of wood materials in forest industry, by improving the greenhouse-type dryer or solar house-type dryer, several highly advanced models of solar lumber drying apparatus were provided and structured. A test of performance of one of them was carried out successfully at the experimental site in Hokkaido. In this case, practical use of solar radiation under a new concept of transparent insulation-blackbody cavity effect, two models of a fully passive-type solar lumber drying house were designed and constructed. One of which is a south-north model and the other is an east-west model. The measurement and analysis on the working performance of both models were carried out by our project team for several years under severe winter season. The results obtained from both models were fairly good and compared well with each other. Consequently, from the performance, both models of the fully passive solar lumber drying house developed, in this national project, were recognized to be good for drying laminar lumber, even under a sever cold season in Hokkaido.

This research is based on a new concept, therefore, a special feature involved in the article, will be expressed by a few technical keywords which will introduce the contents as follows: (1) transparent insulation/blackbody cavity effect, (2) composite surface, (3) CF-sheet, (4) coefficient of transmittance-absorptance, (5) volumetric S. R. incidence, (6) efficiency of volumetric solar heat collection, (7) volumetric solar heat collected, (8) insulated cylinder (chimney), (9) thermo siphon effect, and so on.

1.1 Short historical overview on the related researches

For several decades until this time in Japan, the researches on a solar lumber drying apparatus are mainly as follows: (1) Firstly, a small sized semi passive-type solar lumber dryer made by hand was experimented by Hokkaido Forest Research Institute (Norota, T., et al., 1983) and some products were practically used over northern area in Hokkaido. (2) Second, a large scale solar lumber drying house, an active-type, was developed by a big company, as a national project (Miyoshi, M., Sep., 1987), (Kanayama, K., Baba, H., 2004), and was examined for three years. (3) Third, as a result of the above task, a larger one, using the same type of apparatus was constructed by technical transfer to overseas. In Indonesia, a much bigger size active-type solar lumber drying system was constructed for drying a broadleaf wood, like lauan, during several year (Yamada, M., 1998).

However, in this research aimed at solar lumber drying by improving an agricultural vinyl house, an active-passive type was examined (Kanayama, K., et al., 2006), adopting the new concept as above, and "a fully passive-type solar lumber drying" was ultimately created by our project team (Kanayama, K., et al., 2007), (Kanayama, K., et al., 2008), (Baba, H., et al., 2008). This technical article (Kanayama, K., et al., 2009), (Baba, H., et al. 2009), firstly deals with an optical-thermal mechanism of volumetric solar radiation (S. R.) incidence and a capability of volumetric solar heat collected into "a fully passive-type solar lumber drying house" covered by a composite film, consisting of a triple transparent film and a CF-sheet. The outside view of "a fully passive-type solar lumber drying house" looks like non-transparent from the outside, so it might be called an opaque house. An insulated cylinder (chimney) with a damper duct is set on the outside of the opaque house to make it fully passive function. Subsequently, the opaque house was carefully designed and actually constructed at the main site for the proving test; Ashoro (43°14.5′N, 143°33.5′E) and the sub-site for the proving test, Asahikawa (43°46′N, 142°22′E) in the eastern and northern parts of Hokkaido respectively. A proving performance test of the opaque house and the analysis of the results were successfully carried out by our project team for two and a half years. The capability of the solar lumber drying of the opaque house could be verified experimentally (Kanayama, et al., Aug., 2008), (Baba. et al., Oct., 2008), (Koga, et al., Oct., 2008).

2. A new concept of a solar lumber drying technology

2.1 Outline of the concept

An opaque house is covered by a composite surface consisting of a triple transparent film with double air layers and a CF-sheet, among which are a few spaces held by a skeleton frame. In this case, solar radiation (S. R.) incident upon the house surface is absorbed by the CF-sheet effectively, and converted into solar heat (infrared radiation) and only few

part of the incidence is transmitted through the opaque house as solar ray ultimately. As shown in Fig.1, this optical and thermal mechanism is induced by a "transparent insulation/blackbody cavity effect" (Kanayama, K., et al., 2010), (Kanayama, K., et al., 2010). From this, an incident ray falls three-dimensionally into the cubical opaque house (=Volumetric S. R. incidence) and global S. R. from the sky is collected three-dimensionally by the opaque house (=Volumetric solar heat collected) too. In this case solar heat can be collected passively by the opaque house and saved passively into the opaque house. Hence, any electric power is needless. On the other hand, a moist air produced when drying lumber in the opaque house can be sucked by the draft force through an insulated cylinder set on the outside of the opaque house (Fig.5). This is a thermo siphon phenomenon caused by density difference due to temperature difference between inside air and outside air of the opaque house. As above, the combination of the composite surface consisting of a triple transparent film and a CF-sheet, and an insulated cylinder with a damper duct, could successfully collect S. R. Besides, the inside air is taken out from, and the outside air is taken into, the opaque house in accompany of the phenomenon. In this case, electric power is needless, so this is the reason for the name: "a fully passive-type solar lumber drying house".
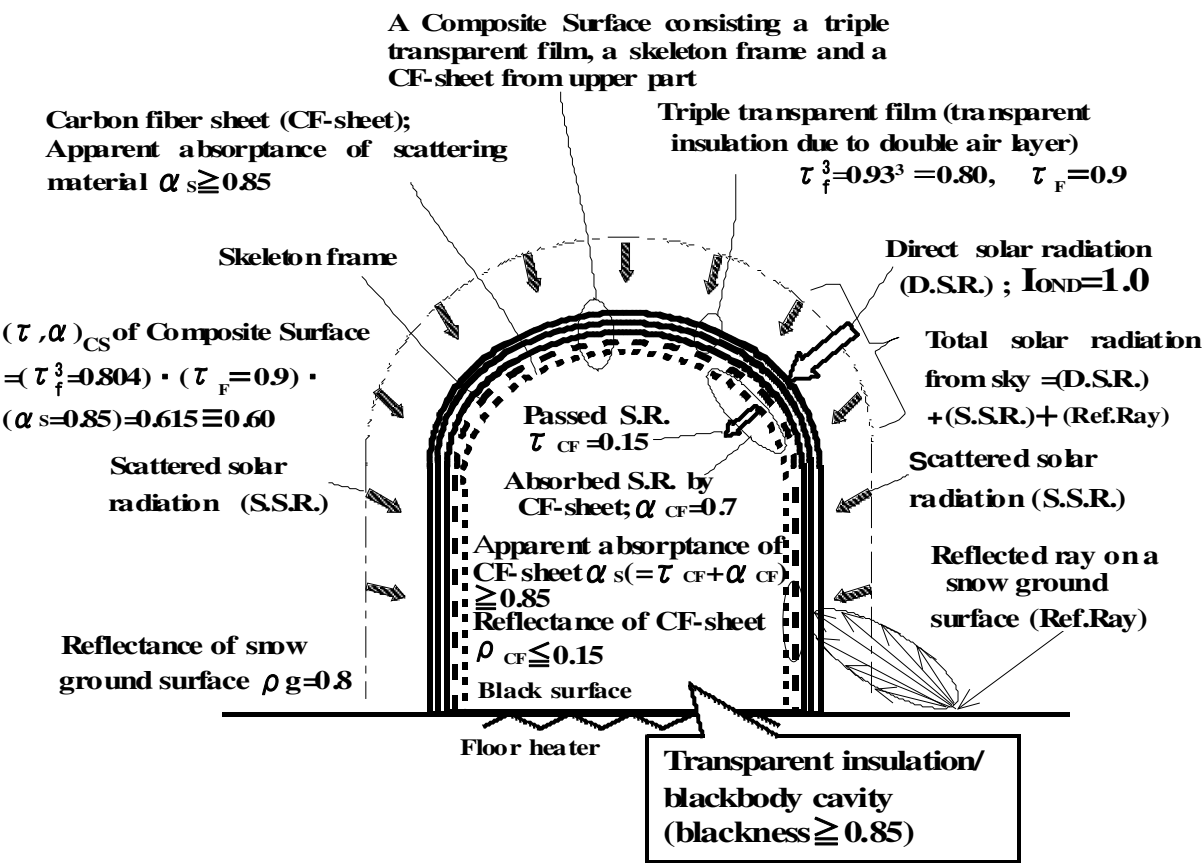

Fig. 1. "Transparent Insulation/Blackbody Cavity Effect" on the opaque house covered by a composite surface. (Kanayama, K. et al., Jun., 2009)

2.2 Explanation on the "transparent insulation/blackbody cavity effect"

Referring to Fig.1 and Fig.2, when a unit of S. R., Io_{ND} (Normal direct radiation=1.0), was incident upon the opaque house covered by a composite surface, 0.804 of that is transmitted through triple transparent film, 0.85 of that is absorbed by the CF-sheet (=scattering medium with apparent absorptance 0.85), and 0.9 of that is passed through a skeleton frame, as discussed in the section 2.3 in detail. However, the CF-sheet inside the house absorbs 0.7, transmits 0.15, and the residual 0.15 is reflected toward the outside of the opaque house. Consequently, 0.615 ($\equiv$0.6) is trapped as solar heat (=infrared radiation) into the opaque house. Because the inside of the house is a closed space covered by the composite surface involving the CF-sheet, the solar heat under goes secondary reflection, absorption and re-emission as infrared ray in the cavity, so that a quasi-blackbody is realized or obtained with blackness of 0.85 or more, because that the transmitted ray of 0.15 is also incident on any body inside the house, and absorbed as heat.

A component transmitted outside from the inside of the house is very small due to triple transparent film, but mostly opaque for the infrared region. Heat (=near infrared and infrared radiation) of relatively high temperature inside the house is mostly, sometimes, shut out by the double air layers among the triple film, and due to a radiation property which is protective for infrared region, so that as a result, heat transfer loss is negligibly small. Thus, when S. R. is incident upon an opaque house it is mostly trapped within the opaque house as solar heat. Therefore, this phenomenon, because that the inside of the house is filled with infrared radiation beam, is called "transparent insulation/blackbody cavity effect".

2.3 Component materials and efficiency of volumetric collection

Fig.2 shows relation between radiation properties of the materials, consisting of composite surface, and intensity of direct S. R. incidence Io_{ND} in detail. On the radiation property of each material, assuming that a single transparent film's transmittance is τ_f=0.93, a triple transparent film's transmittance is τ_f^3=0.804. If the CF-sheet's absorptance is α_S=0.85, and the passing rate of the skeleton frame is τ_F=0.90, so the coefficient of transmittance-absorptance of the composite surface becomes $(\tau \cdot \alpha)_{CS}=\tau_f^3 \cdot \alpha_s \cdot \tau_F$=0.804・0.85・0.90=0.614$\equiv$0.60. Fig.3 shows angular relation (θ, a) of solar colleting surfaces A_n and a house model, consisting of multi-surface A_n, n=1….n. If the solar radiation (S. R.) incident on the multi-surface, made up of a number of composite surfaces, from A_1 to A_n, was known a intensity of $I(d)_{tilt}$, on a tilt surface, by multiplying the $I(d)_{tilt}$ into the corresponding surfaces, $A_1 \sim A_n$, and summing up each product, the volumetric S. R. incidence, $I(Q)_{VI}$, can be determined. Moreover, by multiplying coefficient of transmittance-absorptance $(\tau \cdot \alpha)_{CS}$ 〔=0. 6〕 into $I(Q)_{VI}$, the volumetric solar heat collected, Q_{VC}, is obtained. This is called as a conventional calculation method. Therefore, the efficiency of volumetric solar heat collected η_{VC} is defined as following Eq.(1):

$$\eta_{VC}=I(Q)_{VI}/I(Q)_{fl}\times(\tau \cdot \alpha)_{CS}=\eta_{VI}\times(\tau \cdot \alpha)_{CS} \tag{1}$$

where $I(Q)_{fl}$ is S. R. incidence on the floor, η_{VI} is the efficiency of the volumetric S. R. incidence. In this case, $I(d)_{tilt}$ in the database (NEDO's Report, (1997)) shown in Table 1 from AMeDAS is used as numerals at the experimental site; Ashoro (43°14.5'N, 143°33.5'E), Tokachi-pref., in Hokkaido.
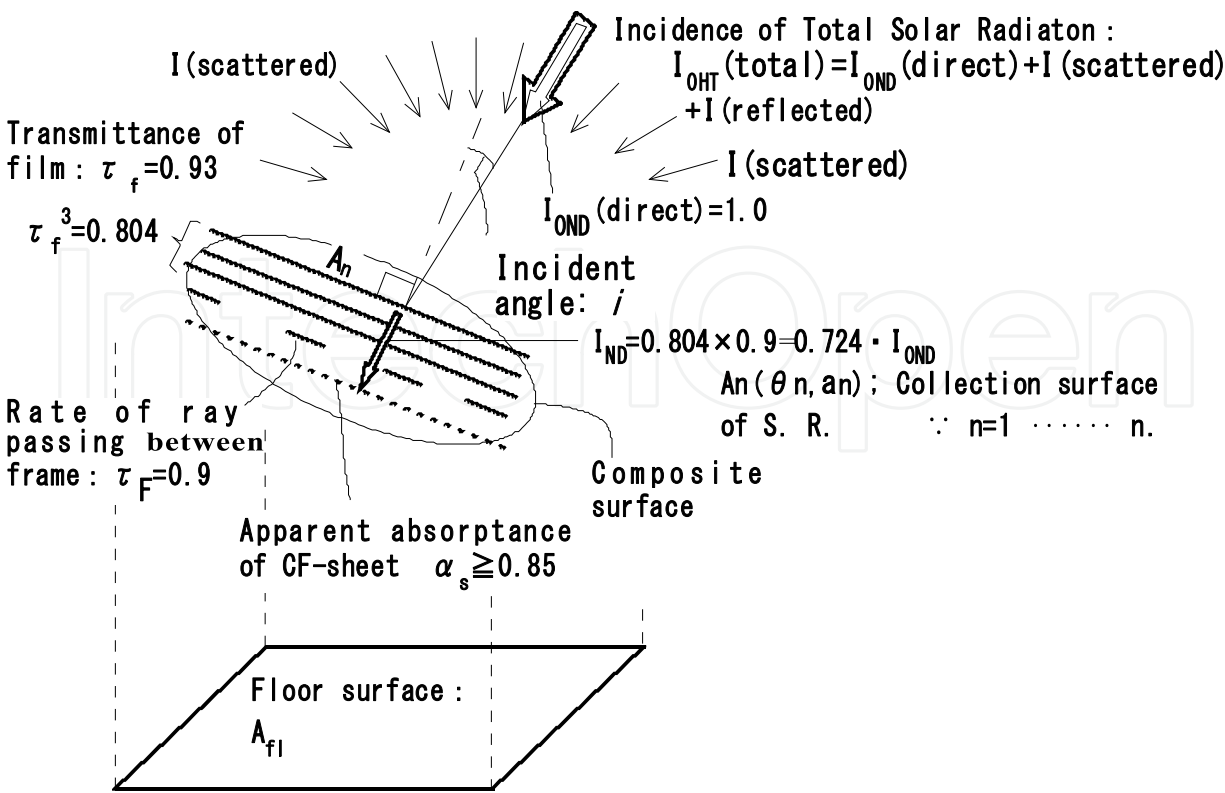
Fig. 2. Radioactive property of materials consisting the house and a mutual relation between incident S. R. and collecting surface
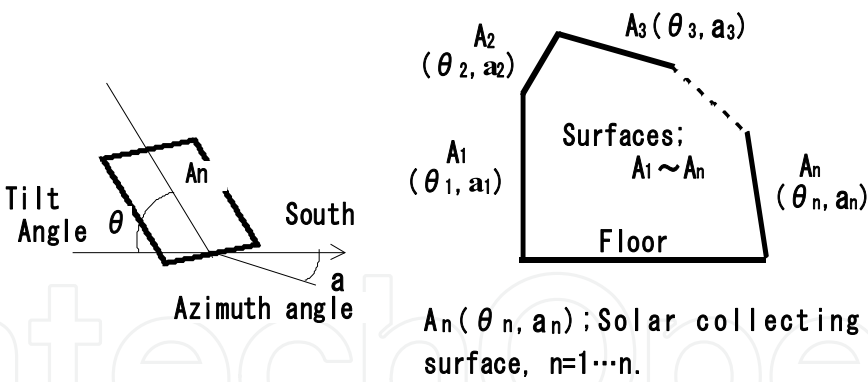

Fig. 3. Angle relation on a solar collecting surface A_n and a house model consisting of multi-surface A_n, n=1···n

Surfaces	Angles of Tilt θ & Azimuth a	Jan	Feb	Mar	Apl	May	Jun	Jly	Aug	Spt	Oct	Nov	Dec	Year
Roof: I(d)rf=I(d)fl=I(d)HT =Horizontal Total S.R.	θ=0°a=0°	6.768	10.15	13.86	15.95	17.75	17.86	15.88	13.82	11.77	9.828	6.696	5.544	12.17
South Surface. ; I(d)ws	θ=90°a=0°	13.46	15.84	14.18	10.33	8.928	8.316	7.956	7.992	8.928	11.23	10.91	11.16	10.76
East-West Surfaces ; I(d)WE/WW	θ=90°a=90°	11.59	17.57	18.58	18.72	20458	19.94	17.64	15.41	14.04	12.89	9.360	8.748	15.41

Table 1. Solar Radiation (S. R.) Incidence on a Tilt Surfaces I(d)tilt at Experimental Site; Ashoro (43°14.5′N, 143°33.5′E) MJ/m²d (South-North model)

3. Calculation method of performance factors by a simplified model of an actual opaque house, (Kanayama, K., et al., Oct., 2008)

As shown in Fig.4, $(\tau \cdot \alpha)_{CS}$ corresponds to an efficiency of collection of volumetric S. R. incident upon the composite surface.

That is, $(\tau \cdot \alpha)_{CS}$ is always constant as 0.6 determined only by a radiation property of material, having no connection with S. R. intensity. In Fig.4, shows the efficiency, η_{AC}, of solar heat collection by a typical flat-type. However, η_{AC} is a function of Io_{ND}, changing in proportion to S. R. intensity.
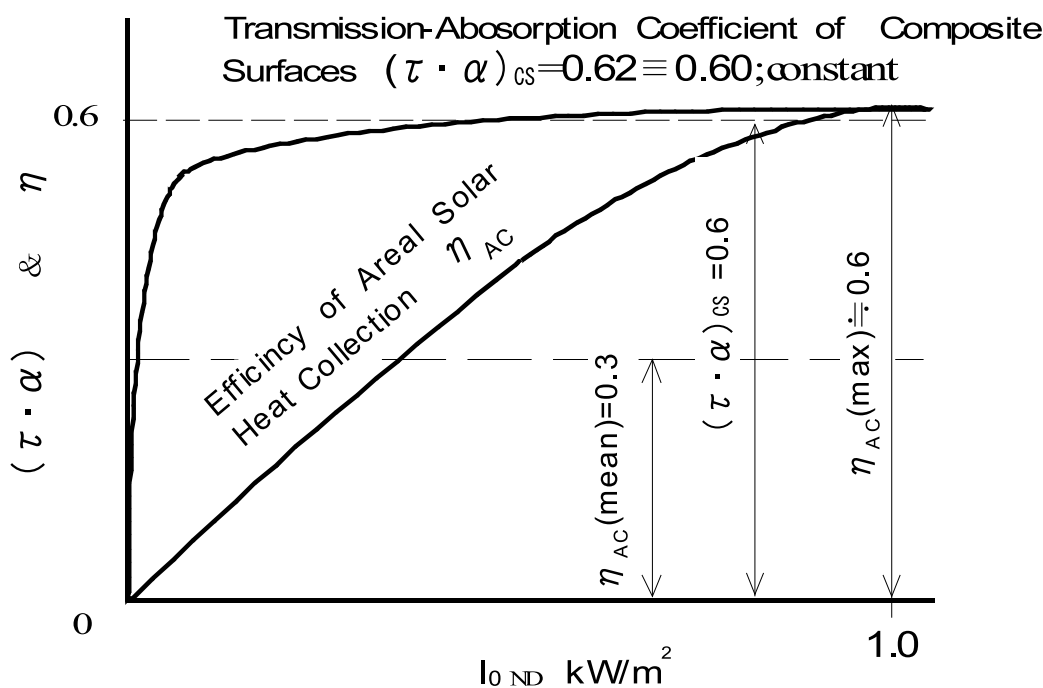

Fig. 4. Transmission-absorption coefficient for volumetric solar heat collection and an efficiency of areal solar heat colection

3.1 On the "South-North model"

On the database shown in Table 1 (NEDO's Report, 1997), $I(d)_{rf}$ is S. R. incident on a roof surface, $I(d)_{ws}$ is S. R. incident on a south wall, $I(d)_{we/ww}$ is S. R. incidence on an east and a west walls, all of which are tilt S. R. incidence per unit surface and per one day (MJ/m²d) in each month respectively. Fig.5 shows a calculation model of an opaque house adopted in the conventional calculation method. The model of the opaque house (South-North model) is shaped a Quonset hut (floor area 5.0 m×5.0 m=25.0 m², height 3.4 m), besides two insulated cylinders which are set vertically outside the house. Thus, all the surfaces of the house is covered by a composite surface consisting of triple transparent film and CF-sheet, so that the actual house looks opaque. As volumetric capacity of the opaque house, can contain stacked lumber of net 10 m³ in maximum to be loaded along south-north direction.
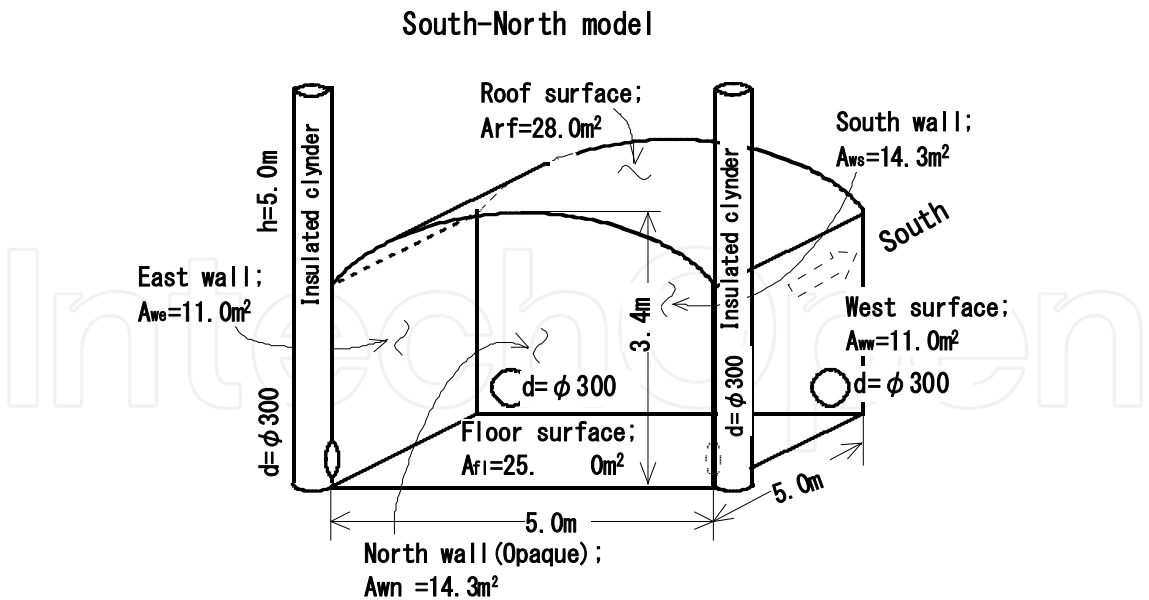
South-North model

Fig. 5. A fully passive solar lumber drying house (South-North model)

Fig.6 shows an estimation, calculated by a conventional method, on the drying performance of the "South-North model" of the opaque house. During the season of spring to early summer, the volumetric solar heat collected Q_{VC} attained between 170～450 MJ/d. The rate of these numerals to S. R. incident on the floor is corresponds to an efficiency of volumetric solar heat collected η_{VC}, which are nearly to 120～200 %. η_{VC} is larger in winter and smaller in summer than yearly averaged value, thus its maximum value is 198 % in January and its yearly averaged value is 139 %.
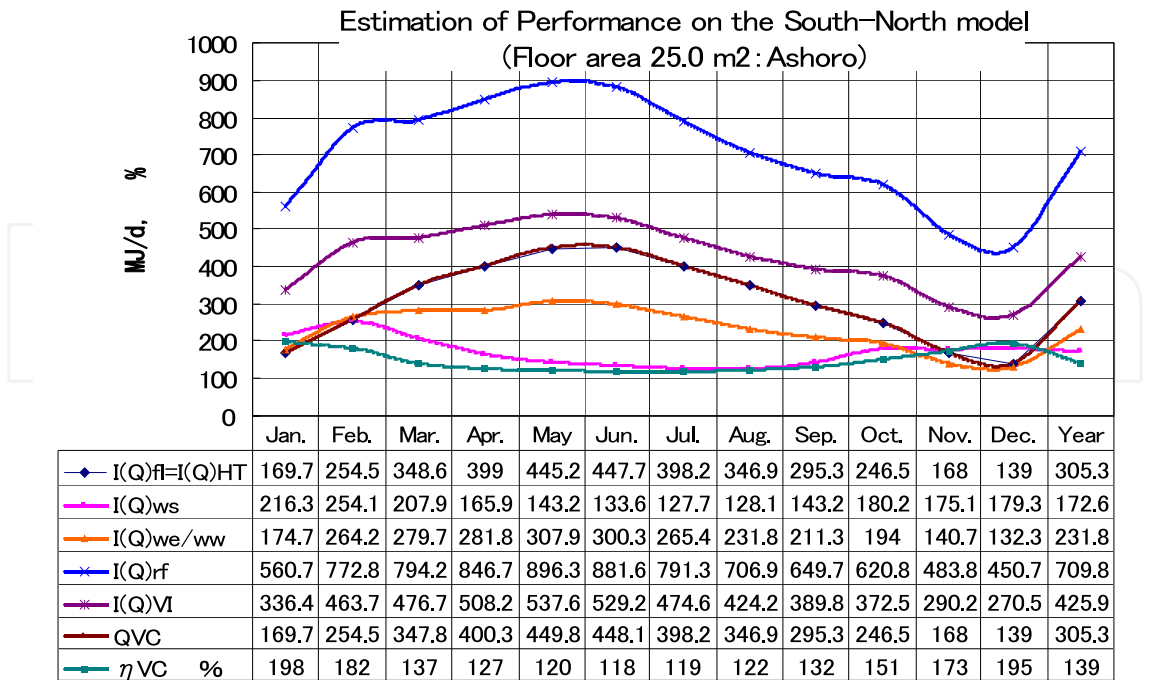
Estimation of Performance on the South-North model
(Floor area 25.0 m2：Ashoro)

	Jan.	Feb.	Mar.	Apr.	May	Jun.	Jul.	Aug.	Sep.	Oct.	Nov.	Dec.	Year
I(Q)fl=I(Q)HT	169.7	254.5	348.6	399	445.2	447.7	398.2	346.9	295.3	246.5	168	139	305.3
I(Q)ws	216.3	254.1	207.9	165.9	143.2	133.6	127.7	128.1	143.2	180.2	175.1	179.3	172.6
I(Q)we/ww	174.7	264.2	279.7	281.8	307.9	300.3	265.4	231.8	211.3	194	140.7	132.3	231.8
I(Q)rf	560.7	772.8	794.2	846.7	896.3	881.6	791.3	706.9	649.7	620.8	483.8	450.7	709.8
I(Q)Vl	336.4	463.7	476.7	508.2	537.6	529.2	474.6	424.2	389.8	372.5	290.2	270.5	425.9
QVC	169.7	254.5	347.8	400.3	449.8	448.1	398.2	346.9	295.3	246.5	168	139	305.3
η VC %	198	182	137	127	120	118	119	122	132	151	173	195	139

Fig. 6. Monthly and yearly estimated performance of the volumetric solar heat collected Q_{vc} and the efficiency of volumetric solar heat collection η_{vc}

3.2 On the "East-West model"

Table 2 shows a database from AMeDAS (NEDO's Report, 1997) at the proving test site. Fig. 7 shows a calculation scheme for the test for the "East-West model" of the opaque house. Similarly from Table 2, on the "South-North model", multiplying the daily S. R. on each tilted surface, per unit area, per day, i.e. $I(d)_{rf}$ on the roof surface, $I(d)_{fl}$ on the floor surface, $I(d)_{ws}$ on the south wall, and $I(d)_{we/ww}$ on east and west walls, by each area; A_{rf} of roof area, A_{fl} of floor area, A_{ws} of south wall, and $A_{we/ww}$ of east and west walls respectively, and by summing up all of them, the volumetric S. R. incidence $I(Q)_{vI}$ can be determined. Then multiplying the product of each term by the coefficient of transmittance-absorptance 0.6, and by summing up all the terms, thus the volumetric solar heat collected Q_{vc} can be determined. The results are shown in Fig. 8 with a data Table. According to the results of Fig 8, an efficiency of volumetric solar heat collection η_{vc} based on solar radiation incident on the floor area, 206 % is maximum in January, 117 % is minimum in June, and 141 % is average value for the year. These are the largest merit in the concept of volumetric solar heat collection.

Surfaces	Angles of Tilt θ & Azimuth a	Jan	Feb	Mar	Apl	May	Jun	Jly	Aug	Spt	Oct	Nov	Dec	Year
Roof S.; $I(d)_{rf}=I(d)_{fl}$ $=I(d)_{HT}$	$\theta=0°$ a=0°	6.768	10.15	13.86	15.95	17.75	17.86	15.88	13.82	11.77	9.828	6.696	5.544	12.17
Roof S.; $I(d)_{rf}=I(d)_{10°}$	$\theta=10°$ a=0°	8.665	12.17	15.61	16.96	18.32	17.92	16.23	14.40	12.72	11.33	8.300	7.202	13.34
South S. ; $I(d)_{ws}$	$\theta=90°$ a=0°	13.46	15.84	14.18	10.33	8.928	8.316	7.956	7.992	8.928	11.23	10.91	11.16	10.76
East-West Ss.; $I(d)_{we/ww}$	$\theta=90°$ a=90°	11.59	17.57	18.58	18.72	20.458	19.94	17.64	15.41	14.04	12.89	9.360	8.748	15.41

Table 2. Solar Radiation (S. R.) Incidence at Experimental Site; Ashoro (43°14.5'N, 143°33.5'E) MJ/m²d (East-West model)
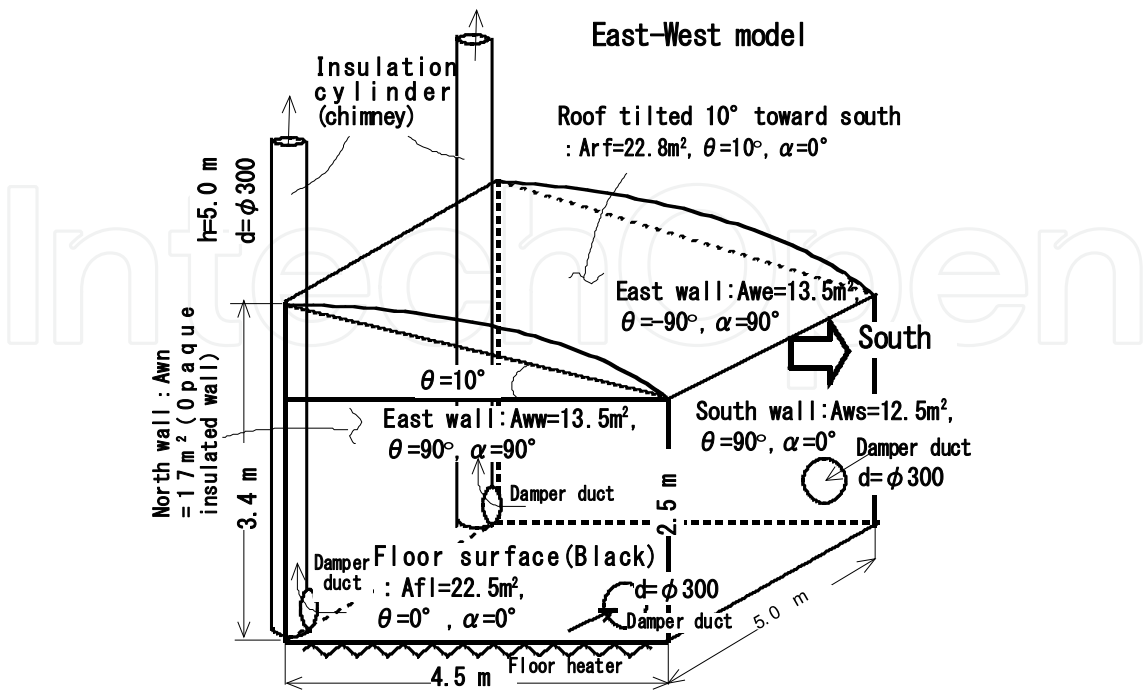

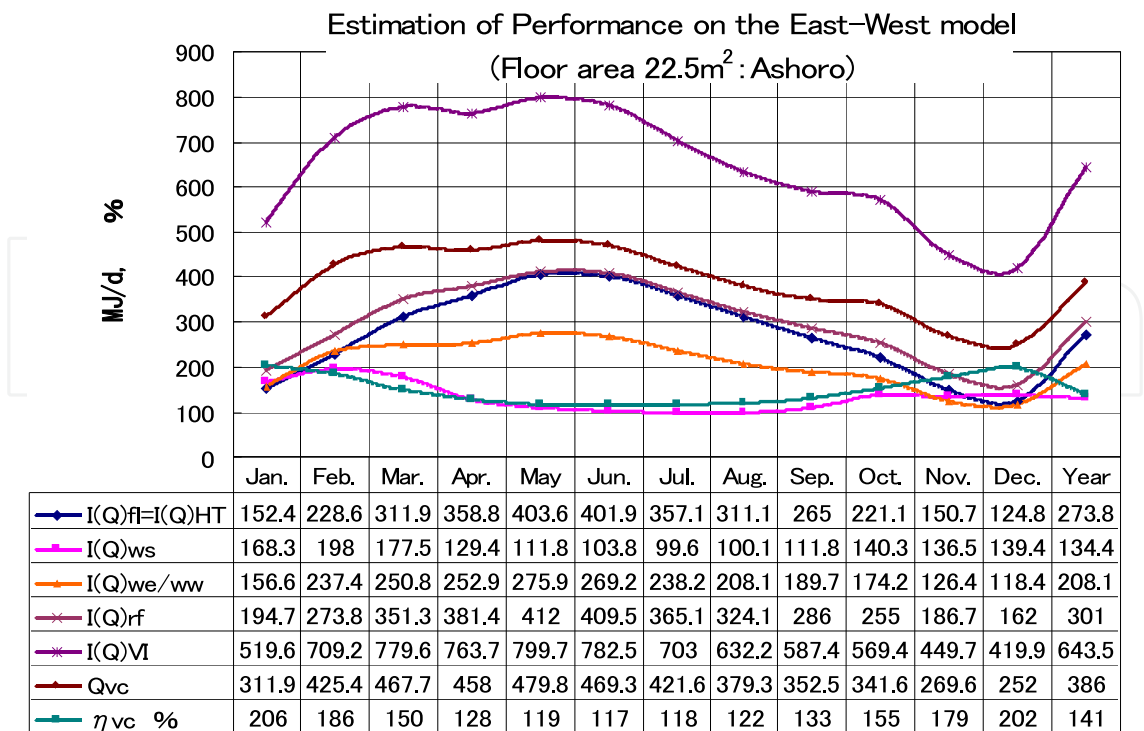Fig. 7. A fully passive solar lumber drying house (East-West model)

Estimation of Performance on the East–West model
(Floor area 22.5m^2 : Ashoro)

	Jan.	Feb.	Mar.	Apr.	May	Jun.	Jul.	Aug.	Sep.	Oct.	Nov.	Dec.	Year
I(Q)fl=I(Q)HT	152.4	228.6	311.9	358.8	403.6	401.9	357.1	311.1	265	221.1	150.7	124.8	273.8
I(Q)ws	168.3	198	177.5	129.4	111.8	103.8	99.6	100.1	111.8	140.3	136.5	139.4	134.4
I(Q)we/ww	156.6	237.4	250.8	252.9	275.9	269.2	238.2	208.1	189.7	174.2	126.4	118.4	208.1
I(Q)rf	194.7	273.8	351.3	381.4	412	409.5	365.1	324.1	286	255	186.7	162	301
I(Q)VI	519.6	709.2	779.6	763.7	799.7	782.5	703	632.2	587.4	569.4	449.7	419.9	643.5
Qvc	311.9	425.4	467.7	458	479.8	469.3	421.6	379.3	352.5	341.6	269.6	252	386
ηvc %	206	186	150	128	119	117	118	122	133	155	179	202	141

Fig. 8. Monthly and yearly estimated performance of the volumetric solar heat collected Q_{vc} and the efficiency of volumetric solar heat collection η_{vc}

4. Performance calculation and proving test of the opaque house

In the previous section, a performance analysis on "South-North model" and "East-West model" of an opaque house was carried out by applying numerals of the database of S. R. incidence and based on the performance factor of volumetric solar heat collected Q_{VC}, the results were discussed and compared each other. In this section, adopting the actual measurements of S. R. incidence at the proving test site, the performance analyses were carried out according to a normal calculation method as following, and then the results obtained were compared with the proving test (Baba, H., et al., 2008).

4.1 Volumetric solar heat collected by a normal calculation method

Applying the authors' separation method (Baba, H., Kanayama, K., July, 1985) for direct-scattered components of S. R. incidence, volumetric S. R. incidence on the opaque house can be calculated, and then the volumetric solar heat collected Q_{VC} can be obtained. This calculation process is fairly complicated, therefore, only an outline of the method will be given as follows: As shown in the left part of Fig.3, assuming tilt angle $\theta_n°$ and azimuth angle $a_n°$ on a tilt surface A_n respectively, the volumetric S. R. incidence $I(H)_{VI}$ upon an opaque house, can be calculated by multiplying S. R. incidence $I(\theta_n, a_n)$ by each tilt surface A_n of simplified model in the right part of Fig.3 and summing up all of each product $A_n \cdot I(\theta_n, a_n)$, n=1,2 · · · n. Therefore, using the same method , on the actual model of the opaque house, volumetric S. R. incidence upon the opaque house $I(H)_{VI}$ can be calculated by Eq.(2), and the volumetric S. R. incidence $I(Q)_{VI}$, and volumetric solar heat collected Q_{VC} of the actual opaque houses in Fig.5 and Fig.7, can be obtained.

$$I(H)_{VI} = A_{rf}I(\theta_{rf}, a_{rf}) + A_{we}I(90, -90) + A_{ws}I(90, 0) + A_{ww}I(90, 90) + A_{wn}I(90, -180) \quad (2)$$

where, the first term, $\cdots\cdot$, and the fifth term of the right hand of Eq. (2), indicate the S. R. incident on the roof surface, on the east wall surface, on the south wall surface, on the west wall surface and on the north wall surface respectively. Where, $I(H)_{VI}$ is volumetric S. R. incidence in kJ/h, $I(\theta, a)$ is S. R. incidence on the tilt surface with setting angles (θ, a) in kJ/m²h. A_{rf} is roof area m², A_{we} is east wall area m², A_{ws} is south wall area m², A_{ww} is west wall area m², and A_{wn} is north wall area m². Now, the S. R. incidence $I(\theta, a)$ on a tilt surface A_{tilt} with setting angle (θ, a) can be calculated from Eq.(3) by substituting Eqs. (4)$\sim$(6) ·

$$I(\theta, a) = I_{ND}\cos i + I_{SC}\frac{(1+\cos\theta)}{2} + \rho_g I_{HT}\frac{(1-\cos\theta)}{2} \quad (3)$$

where, I_{ND} is the direct S. R. incidence kJ/m²h, I_{SC} is the scattering S. R. incidence kJ/m²h, I_{HT} is the horizontal total S. R. incidence kJ/m²h, ρ_g is the reflectance of the earth, i is the incidence angle between incident ray and the normal to the tilt surface. By integrating Eq.(2) from sunrise time to sunset time, we obtained the volumetric S. R. incidence on a tilt surface par day.

$$\cos i = \sin h\cos\theta + \sin\theta\cos h\cos(A - a) \quad (4)$$

$$\sin h = \sin\phi\sin\delta + \cos\phi\cos\delta\cos t \quad (5)$$

$$\sin A = \cos\theta\sin t / \cos h \quad (6)$$

where, h is the solar altitude angle °, A is the solar azimuth angle °, t is solar time in °, φ is the latitude of the site in °, δ is solar declination angle in°.

By the way, the normal calculation method was utilized to calculate the efficiency of volumetric solar heat collection η_{VC} using the real measurements of S. R. incidence at the proving test site; Ashoro, and the results obtained were plotted in Fig.13.

4.2 Solar radiation (S. R.) incidence on each surface, volumetric S. R. incidence and volumetric solar heat collected

A fully passive-type solar lumber drying house has the peculiar characteristics that not only S. R. incidence upon a roof surface, but also the S. R. incidence upon the wall surfaces around the opaque house can be utilized as solar heat collected. Fig.5 shows the calculation schemes of the "South-North model" of the opaque house. (floor area 25.0 m² (=5.0 m×5.0 m), height 3.4 m).

First, using Eq.(3) the S. R. incidence on the roof surface, and on each vertical wall, with every azimuth angle is calculated, and thus the volumetric S. R. incidence $I(H)_{VI}$ is determined by summing up the S. R. incidence upon each surface, and after substituting into Eq.(2) and integrating with the sun shine hour, volumetric S. R. incidence $I(Q)_{VI}$ overall the opaque house can be determined. The volumetric solar heat collected Q_{VC}, can be determined as the product of $I(Q)_{VI}$ and $(\tau \cdot \alpha)_{CS}$ 〔=0.6〕. Where, the roof surface of the Quonset hut is assumed to be a horizontal flat surface for simplification. However, Fig.6 shows the performance factors on the "South-North model" with data table calculated by

the conventional calculation method, using the database of S. R. incidence at the proving test. Also in the same way Fig.7 shows the calculation scheme for the "East-West model", and also Fig.8 is the results on the "East-West model" with data table of the performance factors calculated by the conventional calculation method, using the database as above.

4.3 Photos and drawings of the opaque houses in detail

In order to compare two opaque houses being tested, the details of the relevant parameters, in depth in drawings are presented with Photo 1 and Photo 2, and in Figs.9 and 10. The actual scheme on the "South-North model" of the opaque house and its outside view when loading the stacked lumber on a trolley in Fig.9, and Photo 1, and that of the "East-West model" with its front view of the opaque house in Fig. 10 and Photo 2 respectively. Fig.9 and Fig.10 are the complete formation, dimensions and arrangements of the parts and so on, as shown by the drawings of the front picture and the plan picture in detail of the actual opaque houses, "South-North model" and "East-West model" respectively. In Fig.9, the "South-North model" has one set of two fan-convectors involving a fin-tube heater and a small fan (50 W×2) on the east floor of the house, and one set of four small fans (25 W×4) on the ceiling on the west side, and the same sort of parts and the same numbers as those are on the opposite floor and ceiling. Those two groups of each set are intermittently operated in the opposite direction in half a day in order to circulate uniformly the inside air as a breeze. In Fig.10, the "East-West model" has only one set of two fan-convectors (50 W×2 each) on the south floor of the house, and only one set of four small fans (25 W×4) on the ceiling part on the north side. Moreover, a floor heater (feed pump; 25 W×2) is molded in the black concrete floor, and we can see the stacked lumber (net volume 10 m^3 in max.) in the central part of both houses. The small fan circulates slowly the inside air of the opaque house to increase the drying speed and to dry lumber uniformly. Hence, air speed of 0.2m/sec between the lumbers is sufficient due to the inside of the opaque house is filled with infrared radiation beam. While, the fan-cons and the floor heater contribute to heat supply for drying auxiliary, however, in summer season or in good weather conditions both auxiliary heats are not necessary.

Photo 1. A Fully Passive Solar Lumber Drying House Loading Larch Lumber (2x4 material); (South-North model)
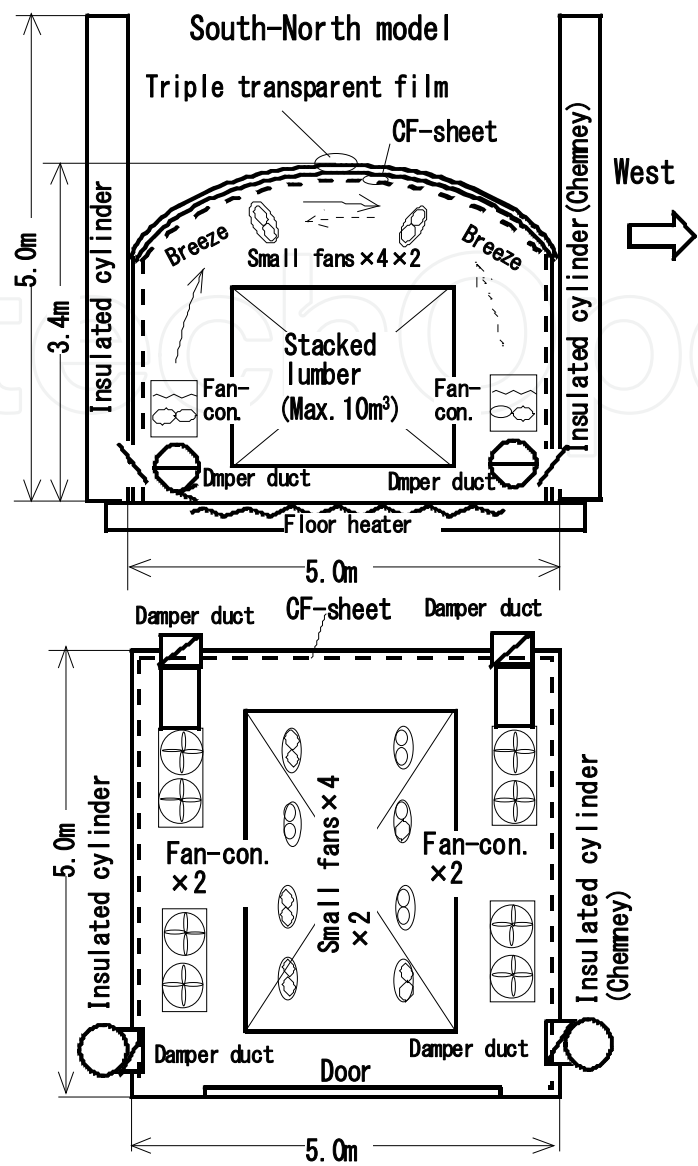
Fig. 9. A Fully Passive Solar Lumber Drying House (South-North model)

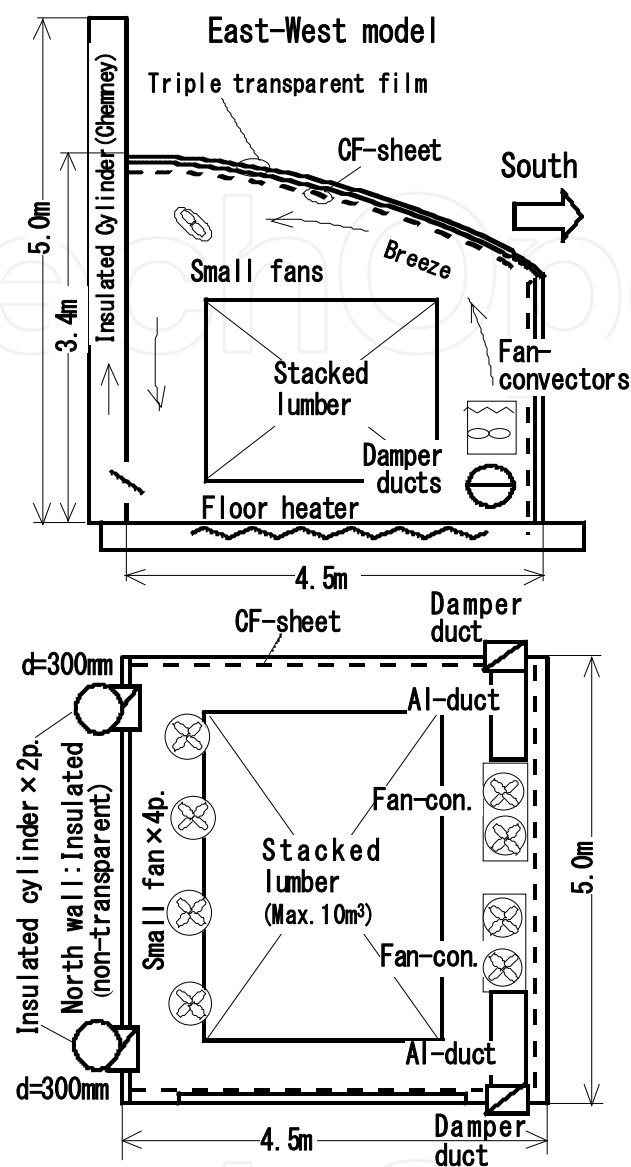Photo 2. Front View of A Fully Passive-type Soalr Lumber Drying House; (East-West model)

Fig. 10. A Fully Passive Solar Lumber Drying House (East-West model)

4.4 Hourly variation of S. R. incidence and solar heat collected, and the others

Fig. 11 shows hourly variations of volumetric S. R. incidence and volumetric solar heat collected over all the opaque house of "South-North model", after obtaining the hourly S. R. incidence on the tilt surface, such as a roof surface and every vertical wall surfaces, applying the normal calculation method to the actual S. R. measurements at the proving test site. In Fig.11, lumber drying test period of fourteen days, between Feb. 19th~Mar. 4th/' 07, in early spring, is a representative graph of several data; two day's graphs on Feb. 23rd (cloudy day) and 24th (fine day) are shown. From this Figure, we can see hourly variation of S. R. incidence on each surface, volumetric S. R. incidence $I(H)_{VI}$ kJ/h, volumetric solar heat collected q_{VC} kJ/h and air velocity in insulated cylinder $V_e\times$ 0.1m/s.
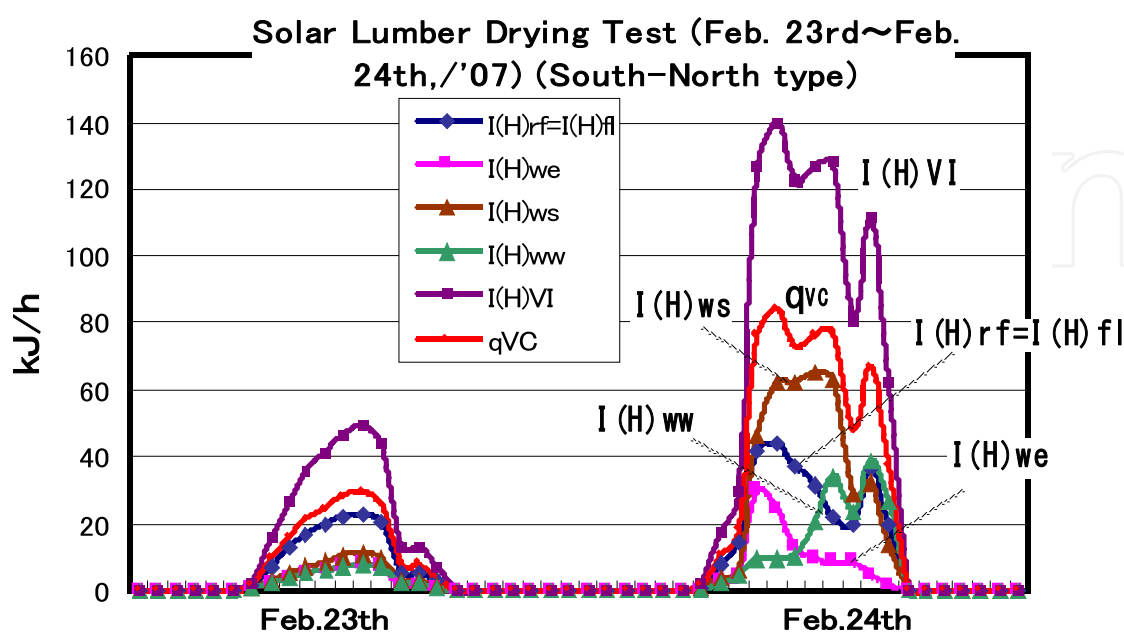
Fig. 11. Hourly variation of the measurement of volumetric S. R. incidence upon each surface and volumetric solar heat collected on cloudy day (23rd) and fine day (24th)

Fig.12 shows hourly variation of all the measured quantities inside and outside the "South-North model" on every day, during the fourteen days of the proving test. Where, T_o is outside temperature ℃, T_i is inside temperature ℃, H_o is outside humidity ％, H_i is inside humidity ％, $I(H)_{HT}$ is horizontal total S.R. incidence $kJ/m^2 h$, V_e is air velocity ×0.1m/s in an insulated cylinder. Outside temperature changes between -20～0 ℃ every day, while the outside humidity changes inversely between 40～90 ％ every day. Inside temperature changes between 35～40 ℃, with average value going slightly up near the end of drying period. Inside humidity is 40～45 ％ initially, however, with progress of lumber drying it gradually goes down to about 10 ％ near the end with varying wavy. Fig.13 shows the estimated efficiency of volumetric solar heat collected $η_{VC}$ of "South-North model" and "East-West model" transferred from Fig.6 and Fig.8. The $η_{VC}$ obtained by the normal calculation method, substituting the measured results of five proving tests during one year, from the first test in Oct. 31st～Nov. 15th/'06 to the fifth test in Aug. 16th～30th/'07 were plotted on the same figure for easy comparison of the quantities. The $η_{VC}$ of "East-West model" is a little greater than that of "South-North model". Moreover, on the former a coincidence between the estimated value and the measured one can be seen. The yearly average estimated value of 140 ％ for "South-North model" is nearly equal to 141 ％ of "East-West model", but on the measured value of 157 ％ for the former, is always greater than 125 ％ of the latter. However, if several simplifications on the calculation process, and characteristics of the field test were considered, these numerical differences could be negligible.
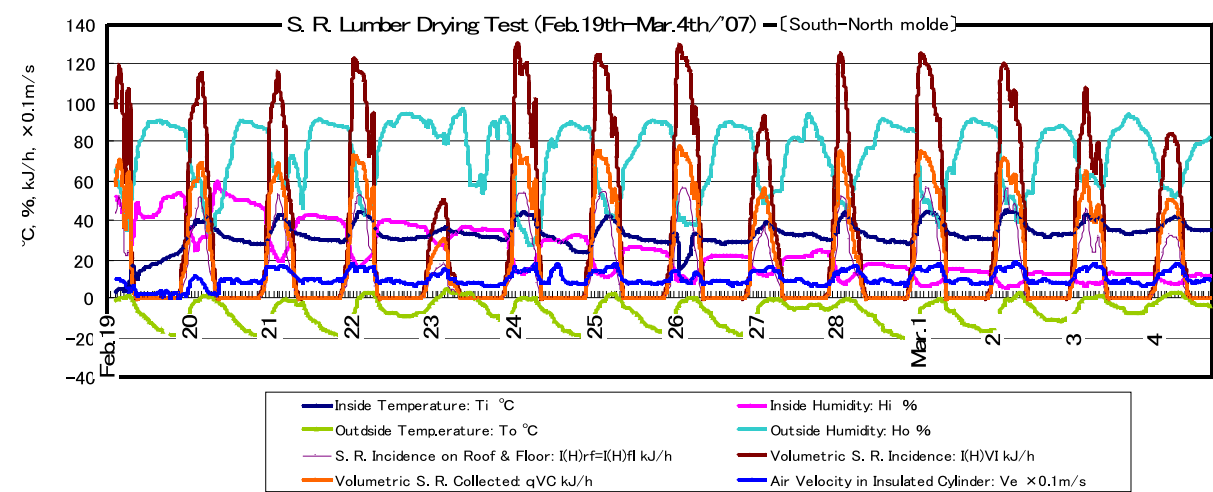
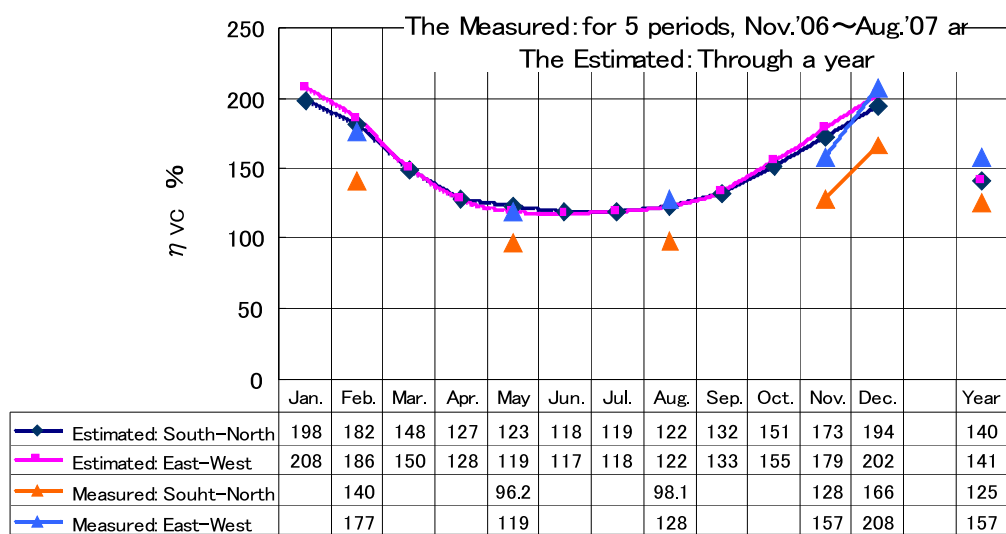Fig. 12. Daily Variation on Main Data Inside and Outside the Solar Lumber Drying

	Jan.	Feb.	Mar.	Apr.	May	Jun.	Jul.	Aug.	Sep.	Oct.	Nov.	Dec.		Year
Estimated: South–North	198	182	148	127	123	118	119	122	132	151	173	194		140
Estimated: East–West	208	186	150	128	119	117	118	122	133	155	179	202		141
Measured: Souht–North		140			96.2			98.1			128	166		125
Measured: East–West		177			119			128			157	208		157

Fig. 13. Comparison betweeen the Estimation and the Measurements of Efficiency of Volumetric Solar Heat Collected η_{vc}

Where, η_{VC} of the "East-West model" appears always to be greater than that of "South-North model", the reason is due to the fact that calculation assumed for the former that the roof surface is 10° tilted toward south as shown in Fig.7, while for the latter, that the surface is horizontal. Table 3 shows the averages of the measurements picked from Fig.10, and the other, from the initial two days and final two days. The difference of air density between the inside and outside of the opaque house, results in the difference of pressure between the inside and outside of the house. As a result, the negative pressure F_d in the insulated cylinder induced by Eq.(7) is a function of the difference of air density γ and the height of insulated cylinder h. The height of the insulated cylinder is 5.0 m and diameter is 300 mm.

$$F_d = h(\gamma_o - \gamma_i) \times 9.8 \ P_a \tag{7}$$

where, $(\gamma_o - \gamma_i)$ is the density difference between inside and outside of the house in kg/m³.

Items	South-North model	East-West model
Outside Temp. T_o / Outside Humid. H_o	−5.0 ℃ /	79.2 %
Inside Temp. T_i / Inside Humid. H_i	36.7℃/13.0 %	37.0℃ /14.0 %
Total Heat Input Q_{in}	21.8 GJ	23.6 GJ
Efficiency of Volumetric Solar Heat Collection η_{VC}	166 %	208 %
Volumetric Solar Heat Collected Q_{VC}	3.6 GJ	4.3 GJ
Solar Heat Fraction F_s	16.4 %	18.3 %
Rate of Evaporation Heat R_{ev}	11.2 %	10.1 %
Water Evaporated W_{ev}	1010 kg	980 kg
Decreas of Moisture Contents ΔM_c	37%→9 % (D.B.)	38%→10 % (D.B.)

Table 3. Experimental Results on the 2nd Drying Test around a Winter Solstice
(Dec. 13th~28th/'06)

The draft force is induced in the insulated cylinder as shown in Fig.12, air velocity in the insulated cylinder goes up over 1m/s when the inside temperature goes up in daytime, and goes down less than 1m/s when the inside temperature goes down at night. Table 3 also specially shows the important results in comparing the opaque houses with each other with their data measured around the winter solstice. The results of the fourth drying test (Feb. 19th~Mar. 4th/'07), in Fig.14, shows the performance factors of both "South-North" and "East-west" by a bar chart graph. S. R. incidence on a floor area of the opaque house, measured at the proving test site, the efficiency of volumetric solar heat collected η_{VC} estimated from the database in March was 140 % for "South-North model"; it was nearly equal to η_{VC}=148%. Thus, the differences in performance factors between "South-North model" and "East-West model" are caused by the fact that the former is a prediction estimated from the past statistics weather data and the latter is that given from a normal calculations using S. R. measured.

Similarly, based on S. R. incidence on the floor area of the opaque house, efficiency of volumetric solar heat collection η_{VI} is 232.4 % for "South-North model" and 294.8 % for "East-West model". The fact that "East-West model" 's efficiency is always larger than that of "South-North model" is caused by assuming that the roof surface of "East-West model" is tilted 10° toward south as described above. Fig.15 (Koga, S., et al. Oct., 2007) shows the result of drying test of larch lumber (2×4 material). Size of the specimen of lumber is 50 mm D×100 mm W×3,650 mm L and number of the specimen is 441 pieces, so that net volume of the stacked lumber is 8 m³. In general, net volume 10m³ of the lumber can be loaded in the opaque house. Larch lumber with initial moisture content 40 % (D.B.) was dried out less than 10% in two weeks, however, the other results of "South-North mode" and "East-West model" are about same with each other. In the case an auxiliary heat was supplied, the solar heat fractions were about same, 30 % in both cases. In summer, lumber drying by only solar heat is capable of drying out less than 20 % within two weeks, during which the solar heat fraction is 100 %. (Koga, S., et al., Oct., 2008)
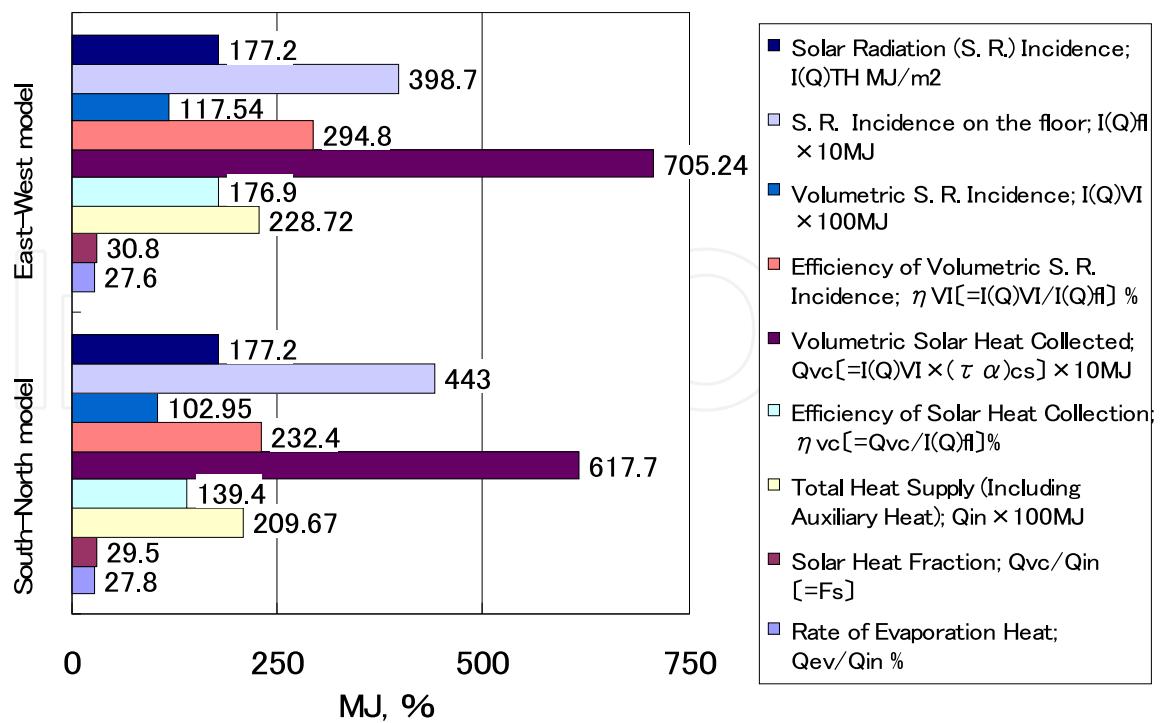
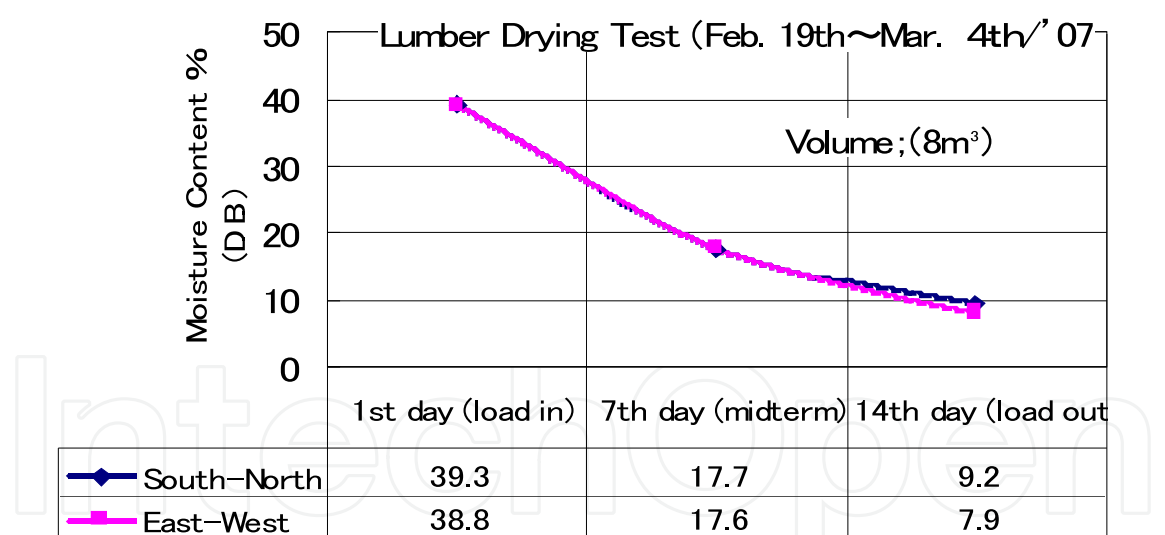Fig. 14. Performance factor on Solar Lumber Drying Test; Feb. 19th~Mar. 4th (2007)

Fig. 15. Comparison of Drying Speed between South-North model & East-West model

4.5 Progression on the working performance of the opaque house

The results of the research on the opaque house, as NEDO's project, carried out at the main site of the proving test; Ashoro, were described mostly. However, in the parallel activity, at the sub-site; Asahikawa, Hokkaido Forest Product Research Institute (HFPRI), which is a member of our project team, in order to grade up the performance of the opaque house, a patient examination has to be continued for more efficient usage, after the expiry of the national project. A technical advantage was found out for the laminar larch lumber, to

produce high quality materials with less moisture distribution and less exude of resin than former (Kanayama, K., et al., Nov., 2010), (Koga, S., et al., Oct. 2008). Moreover, HFPRI is examining now how to dry not only lamina lumber but also large square sectional lumber with high quality as short as possible utilizing solar radiation only, without any auxiliary heat. Good result is expected.

5. Conclusions

First, the optical and the thermal mechanism of volumetric S. R. collection incident upon an opaque house covered by a composite surface were explained. Second, on a "South-North model" and a "East-West model" of the opaque house, under new concept of volumetric solar heat collection, the working performance of the opaque house was calculated applying S. R. database at the proving test site. As a result, one of the performance factors, η_{VC} of both houses, which was defined as efficiency of volumetric solar heat collection, attained 140 % of averaged value through the year. The rate of solar heat collected was 1.4 times of S. R. incident on the floor of the opaque house. Thirdly, applying a normal calculation method, using S. R. measured at the proving test site; Ashoro, a volumetric solar heat collected Q_{VC} of the opaque house constructed on the site was calculated, the proving test on larch lumber drying was carried out in cooperation with all staffs, and drying performance was verified to be good. Where, an electric power was supplied to feed pumps for auxiliary heat and fans to agitate inside air in the opaque house was 400 W maximum which was negligibly small. Thus, a "fully passive-type solar lumber drying house" proposed by us, could be achieved to dry out larch lumber under the conditions of low temperature and low humidity inside the opaque house.

6. Acknowledgements

7. References

Baba, H., Kanayama, K., (July,1985) Studies of Measuring and Estimating of Solar Radiation (2nd Report), *Trans. JSME, B,* Vol.51, No.467, pp. 2451-2456, Tokyo, Japan.

Baba, H., Kanayama, K., Koga, S., Sugawara, T., (Oct.,2008) Development on a Fully Passive Solar Lumber Dying Apparatus (Part 2), *Journal of JSES*, Vol.34, No.5, pp. 57-64, ISSN0388-9564,Tokyo, Japan.

Baba, H., Kanayama, K., Koga, S., Sugawara, T. , (Jun.,2009) Performance Analysis and Proving Test on a Solar Lumber Drying House Covered by a composite Surface, *Proceedings of 46th NHTS of Japan*, pp.505-506, Kyoto, Japan, (CD-ROM) ISSN 1346-1532, G222.

Kanayama, K., Baba, H., (May, 2004) *Utilizing Technology of Solar Energy,* Morikita-Pubisher Ltd, Co., pp.212-214, ISBN 4 -627-94661-9, Tokyo, Japan.

Kanayama, K., Baba, H., Koga, S., Sugawara, T., (Oct., 2006) Developing Research on an Active-Passive type Solar Lumber Drying House, *Proceedings of Renewable Energy 2006*, pp.509-512, O-T-2-2 (CD-ROM), Chiba, Japan.

Kanayama, K., Baba, H., Koga, S., Seto, H., Sugawara, T., (Jul., 2007) Overview on Solar Lumber Drying Apparatus based on New Concept, *Proceedings of 2007 Symp. on Envir. Engg.,* pp.318-321, Osaka, Japan.

Kanayama, K., Baba, H., Koga, S., Sugawara, T., (Aug., 2008) Developing Research on a Fully Passive Solar Lumber Drying Apparatus (Part 1), *Journal of JSES*, Vol.34, No.4, pp. 39-47, ISSN 0388-9564,Tokyo, Japan.

Kanayama, K., Baba, H., Koga, S., Sugawara, T., (Oct., 2008) Developing Research on a Fully Passive Solar Lumber Drying Apparatus—Creation of a new concept and establishment of a soft technology— *Proceedings of Renewable Energy 2008*, O-ST-009, (CD-ROM), Busan, Korea.

Kanayama, K., Baba, H., Koga, S., Sugawara, T., (Jun., 2009) Solar Radiation Incidence and Thermal Analysis on an Opaque House Covered by a Composite Surface, *Proceedings of 46th NHTS of Japan*, pp.507-508, Kyoto, Japan, (CD-ROM). ISSN1346-1532, G223.

Kanayama, K., Baba, H., Koga, S., Sugawara, T., (Jun.-July, 2010), Solar Heat Collected into an Opaque House Covered by Composite Surface in which Lumber Drying, *Proceedings of Renewable Energy 2010,* pp. 1-4, P-Th-1 (CD-ROM), Yokohama, Japan.

Kanayama, K., Baba, H., Koga, S., Sugawara, T., (Oct., 2010) Development Research on a Fully Passive Solar Lumber Drying Apparatus, —Creation of a new concept and establishment of a soft technology—*Current Applied Physics 10* (Oct., 2010), pp.s249-s253, ELSEVIER.

Kanayama, K., Baba, H., Koga, S., Tsuchihashi, H., Seto, H., Sugawara, T., (Nov., 2010), Characteristics on an Opaque Solar Lumber Drying House Covered by a Composite Surface, *Proceedings, of JSES/JWEA Joint Conference 2010,* pp.113-116, Koriyama, Japan.

Koga, S., Ohsaki, S.. Mabuchi, T., Ohgi, D., Cho, K., Yamauchi, K., Baba, H., Seto, H., Kanayama, K., Sugawara, T., (Oct., 2007) Developing Research on a Fully Passive-type Solar Lumber Drying House,—On the basis of experimental results from winter to summer—, (Oct., 2007) *Proceedings of JSES/JWEA Joint Conf. (2007),* pp.185-188, Sapporo, Japan.

Koga, S., Kanayama, K., Baba, H., Sugawara, T., (Oct., 2008) Development on a Fully Passive Solar Lumber Drying Apparatus (Part 3), *Journal of JSES*, Vol.34, No.5, pp. 65-70, ISSN 0388-9564.

Miyoshi, A., (Sep., 1987) Development on a Fixed Heat process-type System, *Report of 7th Task Meeting of Branch,* New Energy Developing Organization (NEDO), pp.140-160, Japan.

NEDO's Report, (1997) Data-Map Relating to Solar Radiation around All the Country Based on the JWA's data, —Indication system of monthly averaged horizontal total S. R./S. R. on a tilt surface—, Ashoro, p.110, (CD-ROM,NP9703), or, http://www.nedo.go.jp/contents/MONSOLA00 (801), Ashoro, Japan.

Norota, T., Chiba, M., Nara, N., (Mar., 1983) Studies on Solar Drying of Lumber, *Report of Hokkaido Forest Products Research Institute*, No.72, pp. 97-125, CODEN:HRSKAC, Asahikawa, Japan,

Yamada, M., (May, 1998) "International Corroboration Research on Solar Energy Utilizing System (Indonesia)", *ENAA Report*, *Engineering No.79,* pp.16-19, Tokyo, Japan.
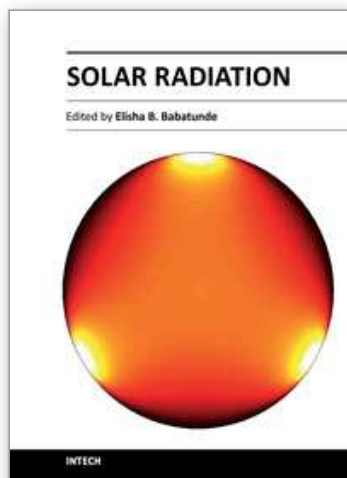
Solar Radiation

Edited by Prof. Elisha B. Babatunde

The book contains fundamentals of solar radiation, its ecological impacts, applications, especially in agriculture, architecture, thermal and electric energy. Chapters are written by numerous experienced scientists in the field from various parts of the world. Apart from chapter one which is the introductory chapter of the book, that gives a general topic insight of the book, there are 24 more chapters that cover various fields of solar radiation. These fields include: Measurements and Analysis of Solar Radiation, Agricultural Application / Bio-effect, Architectural Application, Electricity Generation Application and Thermal Energy Application. This book aims to provide a clear scientific insight on Solar Radiation to scientist and students.

How to reference

In order to correctly reference this scholarly work, feel free to copy and paste the following:

Kanayama Kimio, Koga Shinya, Baba Hiromu and Sugawara Tomoyoshi (2012). An Opaque Solar Lumber Drying House Covered by a Composite Surface, Solar Radiation, Prof. Elisha B. Babatunde (Ed.), ISBN: 978-953-51-0384-4, InTech, Available from: http://www.intechopen.com/books/solar-radiation/an-opaque-solar-lumber-drying-house-covered-by-a-composite-surface

INTECH
open science | open minds